Cell Stress and Chaperones (2015) 20:185–201
DOI 10.1007/s12192-014-0536-1

ORIGINAL PAPER

Celastrol, an oral heat shock activator, ameliorates multiple animal disease models of cell death

Sudhish Sharma · Rachana Mishra · Brandon L. Walker · Savitha Deshmukh · Manuela Zampino · Jay Patel · Mani Anamalai · David Simpson · Ishwar S. Singh · Shalesh Kaushal · Sunjay Kaushal

Received: 5 June 2014 / Revised: 5 August 2014 / Accepted: 8 August 2014 / Published online: 11 October 2014

Abstract Protein homeostatic regulators have been shown to ameliorate single, loss-of-function protein diseases but not to treat broader animal disease models that may involve cell death. Diseases often trigger protein homeostatic instability that disrupts the delicate balance of normal cellular viability. Furthermore, protein homeostatic regulators have been delivered invasively and not with simple oral administration. Here, we report the potent homeostatic abilities of celastrol to promote cell survival, decrease inflammation, and maintain cellular homeostasis in three different disease models of apoptosis and inflammation involving hepatocytes and cardiomyocytes. We show that celastrol significantly recovers the left ventricular function and myocardial remodeling following models of acute myocardial infarction and doxorubicin-induced cardiomyopathy by diminishing infarct size, apoptosis, and inflammation. Celastrol prevents acute liver dysfunction and promotes hepatocyte survival after toxic doses of thioacetamide. Finally, we show that heat shock response (HSR) is necessary and sufficient for the recovery abilities of celastrol. Our observations may have dramatic clinical implications to ameliorate entire disease processes even after cellular injury initiation by using an orally delivered HSR activator.

Keywords Cardiomyopathy · Myocardial infarct · Heat shock response · HSPs · Celastrol

Introduction

Cardiovascular diseases, liver dysfunction, and diabetes are among the leading causes of health care concerns in the world (Minino 2013). Myocardial infarction (MI) leads to myocardial cell death that may progress to fibrosis and dilation of ventricles, all major determinants of cardiac failure. Liver dysfunction is a condition that eventually leads to high mortality rates by causing hepatocyte death and fibrosis. Central to the pathogenesis of these disorders is the activation of inflammatory mediators, reactive oxygen species (ROS), and apoptosis that realigns the delicate balance of cellular viability toward cell death. The timing of cell death may be immediate or delayed depending upon the insult and may be associated with changes in protein homeostasis or proteostasis. Protein homeostasis or proteostasis can be defined as the control of the conformation, concentration, protein–protein interactions, and locations of the individual proteins essential for cell survival (Balch et al. 2008). Both MI and liver dysfunction affect cellular protein homeostasis. Hence, protein homeostatic regulators may counteract and/or reverse these imbalances, prevent further cellular damage, and thus treat the disease process. (Albanese et al. 2006; Balch et al. 2008; Brown et al. 1997; Cohen and Kelly 2003; Deuerling and Bukau 2004; Imai et al. 2003; Kaufman 2002; Mu et al. 2008; Ron and Walter 2007; Young et al. 2004)

Heat shock response (HSR) is a highly conserved ancient process that helps maintain protein homeostasis and is essential for cell survival. (Morimoto 1998; Morimoto and Santoro 1998). Also referred to as the cellular stress response, the HSR is generally characterized by the enhanced expression of heat shock proteins (HSPs), which act as chaperones to maintain

Electronic supplementary material The online version of this article (doi:10.1007/s12192-014-0536-1) contains supplementary material, which is available to authorized users.

S. Sharma · R. Mishra · B. L. Walker · S. Deshmukh · M. Zampino · J. Patel · M. Anamalai · D. Simpson · I. S. Singh · S. Kaushal (✉)
Division of Cardiac Surgery, University of Maryland Medical Center, 110 S. Paca Street, 7th Floor, Baltimore, MD 21201, USA
e-mail: skaushal@smail.umaryland.edu

S. Kaushal (✉)
Retina Specialty Institute, 6717 North 11th Place Suite C, Gainesville, FL 32605, USA
e-mail: skaushal108@gmail.com

proteostasis and protect cells against a wide variety of stressors (Hoogstra-Berends et al. 2012; Niforou et al. 2014). Activation of HSR is mediated by the stress-activated transcription factor heat shock factor-1 (HSF1) in mammals, which, upon sensing stress, is activated to a DNA-binding transcriptional active form. Activation of HSF1 includes trimerization, nuclear translocation, and phosphorylation followed by transcriptional regulation of responsive genes (Morimoto 1998; Shi et al. 1998). Activation of HSR and induction of HSPs have been shown to afford protection in various models of hypoxia, ischemia, and hepatic injury (Dohi et al. 2012; Kubo et al. 2012; Pulitano and Aldrighetti 2008; Tucker et al. 2011). Additionally, overexpression of one or more of the HSPs was shown to protect cells against toxic exposures to diverse stresses, including hydrogen peroxide, toxic chemicals, extreme temperatures, and ethanol-induced toxicity (Huot et al. 1991; Jaattela and Wissing 1992; Jaattela et al. 1992; Lis and Wu 1993; Marber et al. 1995; Mehlen et al. 1995a; Mehlen et al. 1995b; Mestril et al. 1994a; Mestril et al. 1994b; Mizzen and Welch 1988; Morimoto 1993; Mosser et al. 1990; Parsell et al. 1994; Plumier et al. 1995). This has led to studies identifying HSF1-modulating compounds including both inhibitors such as triptolide and quercetin and activators such as puromycin, MG132, radicicol, geldanamycin, and celastrol (Bagatell et al. 2000; Hightower 1980; Holmberg et al. 2000; Jurivich et al. 1992; Lee et al. 1995; Nagai et al. 1995; Westerheide et al. 2006). We originally identified celastrol by a large drug screen study and found that celastrol effects maintenance of cellular proteins by activating HSF1 and affords benefit in a macular degeneration animal model (unpublished data).

Celastrol is a crystalline compound isolated from the root extracts of *Tripterygium wilfordii* (thunder god vine) and *Celastrus regellii* and is a member of the triterpenoid family of compounds which are known for their anti-inflammatory (Jung et al. 2007; Kim et al. 2009a; Kim et al. 2009b; Pinna et al. 2004; Sethi et al. 2007; Trott et al. 2008), anti-tumor (Allison et al. 2001; Chang et al. 2003; Dai et al. 2010), antioxidant (Trott et al. 2008), and heat shock response activation properties (Sethi et al. 2007; Trott et al. 2008; Westerheide et al. 2004). Celastrol acts through multiple mechanisms to exert its biological effect including activation of HSF1 and the HSR, but its effectiveness as a broad regulator and HSR activator to prevent disease processes in in vivo models has not been investigated. In the present study, we analyzed the effect of celastrol in three in vivo mice models involving injury to cardiomyocytes and hepatocytes. We determined whether celastrol rescued the myocardium from doxorubicin (DOX) toxicity or ischemia and thioacetamide (TAA)-induced hepatic injury by examining apoptosis, inflammation, and fibrosis. We also showed that celastrol could effectively activate HSR both in vivo and in vitro, and we propose that the protection afforded by celastrol in myocardial and hepatic injury models is due to its ability to activate the HSR and restore/maintain protein homeostasis.

Materials and methods

Animal studies

Wild-type mice (C57BL/6J) of 6–8 weeks age were purchased from Jackson Laboratories. Animals used in these studies were maintained according to protocols approved by the Institutional Animal Care and Use Committee (IACUC) at Children's Memorial Research Center, Chicago, and University of Maryland, Baltimore.

Reagents and antibodies

Celastrol was purchased from Cayman Chemical, Inc., and stock solutions were prepared in dimethyl sulfoxide (DMSO) at a concentration of 10 mg/ml. In vitro MTT-based toxicology assay kit (TOX-1), doxorubicin, thioacetamide (TAA), triptolide (TTD), and acetaminophen (APAP) were purchased from Sigma, Inc. Terminal deoxynucleotidyl transferase dUTP nick end labeling (TUNEL) assay kit was purchased from Millipore, Inc. For Western blot analysis, hsf1, hsp90, hsp70, hsp40, hsp27 (Enzo Life Sciences), GAPDH, GATA4 (BD Biosciences), cleaved caspase-3 (Cell Signaling), and CD68 (Abcam, Cambridge, USA) primary antibodies were used.

In vivo mouse model of DOX-induced cardiotoxicity

Male C57BL/6J mice were randomly divided into four groups (n=6): control (CNT), only celastrol (CEL) administration, only doxorubicin (DOX) administration, and celastrol and doxorubicin administration (DOX + CEL). At day 0, the DOX group received a single dose of DOX at 20 mg/kg. In the DOX + CEL group, mice received an initial dose of celastrol (4 mg/kg of body weight, i.p.) diluted in 0.1 ml of vehicle (70 % Cremophor/ethanol 3:1, 20 % PBS, and 10 % DMSO) by oral gavage (20 gauge animal feeding needle), 12 h before intraperitoneal injection of doxorubicin (20 mg/kg). The CNT and CEL groups were administered one dose of vehicle by itself and CEL, respectively, by oral gavages every day for 7 days. Animal viability and weight was recorded daily for 5 days. For other animal studies, TTD (0.2 mg/kg/day) or DMSO was delivered by intraperitoneal injections. Animal viability was calculated by survival curve (%) analyzed using GraphPad Prism®.

Myocardial infarction

Mice were randomly divided into four groups: CNT, CEL, MI, and MI + CEL. Animals were anesthetized with 5 % isoflurane in pure oxygen. After endotracheal intubation and initiation of ventilation, isoflurane was reduced to the amount required to prevent the pedal reflex (1.5–2 %). The heart was exposed via a left thoracotomy, and the proximal left anterior descending (LAD) was ligated using 8-0 silk sutures. Buprenorphine (0.1 mg/kg) was injected subcutaneously after surgery (and as necessary), and animals were allowed to recover under close supervision. CEL was administered 6 h prior to LAD ligation in the MI + CEL and CEL groups and every day until the mice were sacrificed (28 days). The CNT and MI groups were administered vehicle.

Induction of hepatic failure

Mice were randomly divided into four groups: CNT, CEL, TAA, TAA + CEL. TAA was dissolved in sterile normal saline (NS) solution and was injected i.p. as a single dose of 500 mg/kg in the TAA (n=6) and TAA + CEL (n=6) groups. Mice in the TAA + CEL group received CEL by oral gavage 24 h prior to TAA injection and every day for 7 days. The CNT (n=5) and (n=6) CEL groups were administered one dose of vehicle by itself and CEL by oral gavages every day for 7 days. Twenty-four hours after injection of TAA, all mice were injected s.c. with 0.5 ml of a solution containing 0.45 % NaCl, 5 % dextrose, and 0.2 % KCl in order to prevent hypervolemia, hypokalemia, and hypoglycemia. The mice were intermittently exposed to infrared light in order to prevent hypothermia.

Histology

Specimens were fixed and processed using standard methods. The sections were stained for hematoxylin and eosin stain. Cryostat sections (7 to 10 μm) were stained with primary antibodies as noted and secondary Alexa Fluor-conjugated antibodies. Staining without primary antibodies was used as control for non-specific fluorescence. TUNEL staining (Millipore, Inc.) for apoptosis in liver and heart tissues was carried out as per the manufacturer's instructions. Immunostained sections were examined by confocal microscopy, and the number of labeled cells was determined as a percentage of the total 4′,6-diamidino-2-phenylindole (DAPI)-labeled nuclei. Infarct size in heart tissue was calculated using Masson's trichrome staining. Briefly, the midline technique for infarct size determination was used as described previously (Mishra et al. 2011). The LV midline was drawn at the center of the anterior (lateral) wall along the length of the infarct. This circumference was divided by the total midline circumference of the heart to determine infarct size. Six sections per animal and six animals per group were analyzed. For cardiomyopathy scoring, blinded investigators evaluated the severity of myocardial damage on a score of 0–3 according to the percentage of vacuolization and myofibrillar loss in five randomly selected areas of each section and three sections per heart tissue (Li et al. 2006).

Echocardiography

Transthoracic echocardiograms were performed on mice using a VisualSonics Vevo 770 ultrasound unit (VisualSonics, Toronto, Canada). The VisualSonics RMV 716 Scanhead with a center frequency of 17.5 MHz, a frequency band of 11.5–23.5 MHz, and a focal length of 17.5 mm was used for echo acquisition in mice. Baseline echocardiograms were acquired 24 h prior to MI with additional echocardiograms acquired at 7 and 28 days post-MI. The animals were maintained lightly anesthetized during the procedure with 1.5 % isoflurane delivered through a face mask. The animals were kept warm on a heating pad, and the body temperature was continuously monitored using a rectal thermometer, maintaining it at 37 °C by adjusting the distance of a heating lamp. Under these conditions, the animals' heart rate could be maintained between 300 and 400 beats per minute. Images were obtained in M-mode from the parasternal short axis at the mid-papillary level to acquire fractional area change (FAC). The images were obtained in triplicate by an echocardiographer who was blinded to the treatment group.

Gene expression analysis

Total RNA was isolated from cells or tissues using RNeasy Kit (Qiagen) according to the manufacturer's instructions. Isolated RNA was reverse-transcribed using oligo-dT primers and a cDNA synthesis kit according to the manufacturer's protocol (Applied Biosystems). Duplicate 20-μl real-time PCR reactions were performed in 96-well plates using a Fast SYBR Green reaction mix using 7500 system or StepOnePlus® (Applied Biosystems). The following PCR conditions were used: initial denaturation at 95 °C for 20 s, followed by 40 cycles of 3 s at 95 °C and 45 s at 60 °C. The C_T values of the housekeeping gene (18s) were subtracted from the correspondent gene of interest (ΔC_T). The fold of expression of each gene in samples treated with drugs or otherwise was determine by the expression $2^{-\Delta\Delta C_T}$. The final values were averaged and results were represented as fold expression with the standard error (triplicates). HSF1 and GATA4 genes were amplified with the primers purchased from Qiagen, Inc. Gene expression levels of IL-1β, IL-6, TNF-α, and MMP2 were quantified in the zone of infarct using QuantiTect Primer Assays (Qiagen, Valencia, CA).

Cell culture and drugs

H9c2 and Huh7 cell lines were purchased from ATCC. Mouse embryonic fibroblasts (MEFs) $HSF^{-/-}$ and MEF $HSF^{+/+}$ were kindly provided by Dr. Ivor Benjamin (Medical College of Wisconsin, Milwaukee, WI). Cells were maintained in DMEM supplemented with 10 % fetal bovine serum and 1 % (*v*/*v*) streptomycin/penicillin at 37 °C in 5 % CO_2 with 90 % humidity. CEL and TTD were dissolved in DMSO at the concentration of 1.0 mM, DOX was dissolved at 1 mmol/l in normal saline, TAA solution was freshly prepared in water at 50 mmol/l, and APAP was dissolved in 70 % ethanol at 10 mM stock concentration. Drugs were added to cells at the indicated concentrations. Cells were treated either with medium containing an equal amount of DMSO or saline to serve as controls.

Flow cytometry

Cell death was measured by FITC Annexin V Apoptosis Detection Kit (BD Biosciences) using flow cytometry. Apoptosis was also detected by measuring active caspase-3 expression. Briefly, the cells were grown as a monolayer and, after fixation and permeabilization, stained with FITC-labeled anti-caspase-3 antibodies (BD Biosciences) according to the standard procedures and manufacturer's instruction.

Immunoblots

After indicated drug treatments, cells were lysed with the RIPA buffer (20 mM Tris-HCl (pH 7.5), 150 mM NaCl, 2.5 mM sodium pyrophosphate, 1 mM Na_2EDTA, 1 mM EGTA, 1 % NP-40, 1 % sodium deoxycholate, 1 mM beta-glycerophosphate, 1 mM Na_3VO_4, 1 μg/ml leupeptin; Cell Signaling Technology®) containing complete protease inhibitor cocktail (Roche Applied Science). Cell lysate was prepared and protein concentration was determined using the BCA method (Thermo Scientific). Forty micrograms of protein lysate was resolved on 4–12 % SDS-PAGE, transferred to a PVDF membrane using a semidry or wet transfer method, and probed with indicated specific antibodies. The membrane was probed with antibodies as needed. The immunoblots were analyzed by Gel Logic 440 or Odyssey system from LI-COR Biosciences for detection and quantitative analysis.

Statistical analysis

Data are presented as mean and error bars depict the standard error of the mean (sem). Data were analyzed using GraphPad Prism 5 software. When comparing two conditions, Student's *t* test non-parametric (Mann–Whitney's) test was used. More than two comparisons were made using one-way ANOVA (non-parametric) with Kruskal–Wallis test followed by Dunn's post hoc test. Western blotting data sets were analyzed by repeated measures ANOVA with Bonferroni's post hoc test. Echocardiography data was analyzed using two-way ANOVA followed by Bonferroni's post hoc test. Probability values of less than 0.05 were considered significant and tests were performed two-sided.

Results

Celastrol is cytoprotective against DOX-induced cardiotoxicity in mice

We tested whether CEL has a cytoprotective effect in a DOX-induced cardiomyopathy model. At day 4, mice treated with a single dose of DOX (n=4; 14.75±0.5 g) had significantly reduced body weights as compared to control untreated mice (n=4; 20.0±0.5 g) (Fig. 1a). Mice treated with CEL (CEL + DOX group) exhibited a decrease in their weights for 3 days (n=4; 16.3±1.0 g), suggesting the DOX insult; however, these mice regained their weight during the next 3 days (n=4; 18.0±1.1 g) to the similar levels as their pretreatment weight. After 7 days post-treatment, DOX treatment of mice resulted in 80 % death while co-treatment with CEL reduced the mortality to only 20 % (Fig. 1b). Mice in the CNT and CEL treatment groups were consistently at 100 % survival rate. We further analyzed the change in functional properties of the heart after 5 days post-DOX treatment. Echocardiography showed that DOX treatment significantly reduced stroke volume, heart rate, cardiac output, and LVEDD, while co-treatment with CEL significantly restored these parameters (Supplemental Fig. 1). On physical examination, a gradual reduction in heart rate was appreciated in the DOX group when compared to the CNT group but increased heart rates were observed in the CEL + DOX group to signify their compensatory response to DOX treatment. These results suggested that the improved survival and cardiac function correlated with CEL treatment in the DOX-induced mortality, which was correlated with mitigation of cardiac dysfunction.

At the macroscopic level, smaller heart sizes were observed in the DOX group at post-treatment day 5, as compared to the CEL + DOX group or the CNT group. The histological findings showed altered myocardial morphology with changes arising in cellular organization: lose myofibrillar and cytoplasmic vacuolization in the DOX group (Fig. 1c). In contrast, these histological changes were not observed in the myocardium of the CEL + DOX group. A comprehensive cardiomyopathy score that examined the incidence and severity of the myocardium was calculated (Li et al. 2006) (Fig. 1d). The DOX group showed significant higher severity cardiomyopathy scores when compared to the scores from the CNT group or from the CEL + DOX group. No cardiomyocyte pathology was observed in the CNT or the CEL group. To investigate

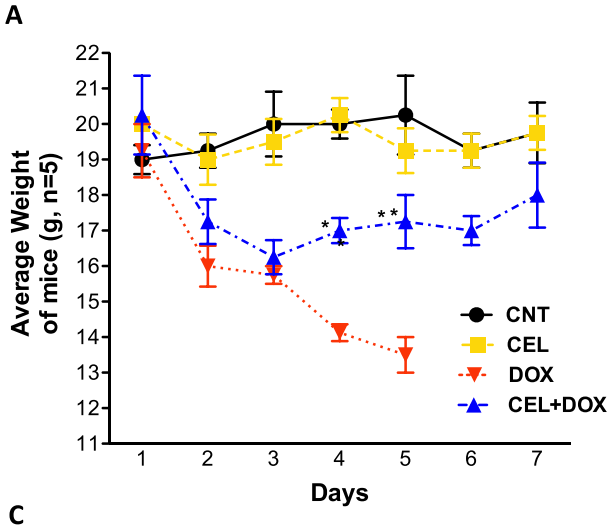

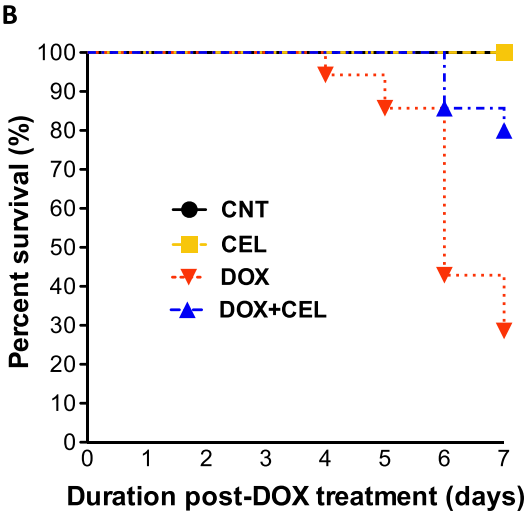

C

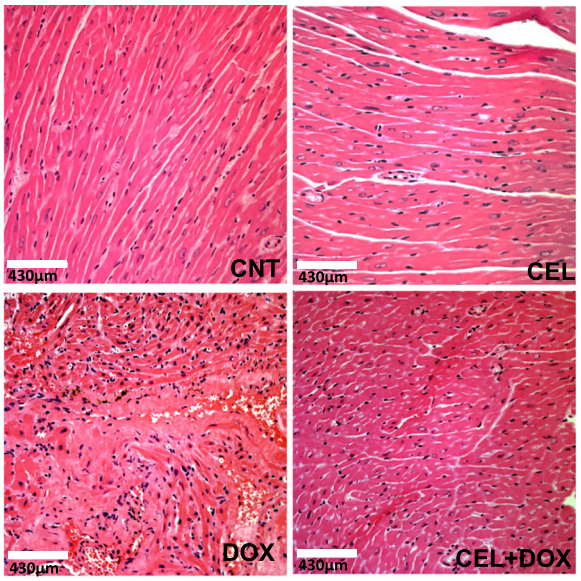

D

CARDIOMYOPATHY SCORE

GROUP	NO. OF ANIMALS	0	1	1.5	2	2.5	3
CNT	14	14	0	0	0	0	0
DOX*	15	0	0	1	3	5	6
DOX + CEL**	13	0	4	7	2	0	0
CEL	12	12	0	0	0	0	0

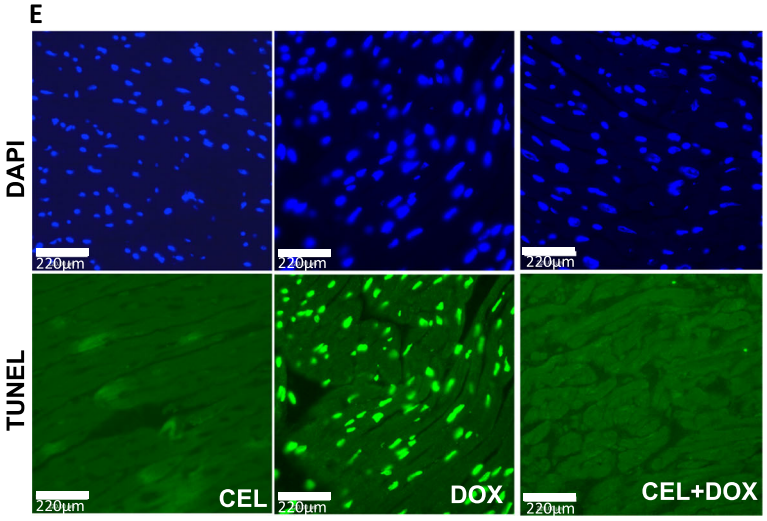

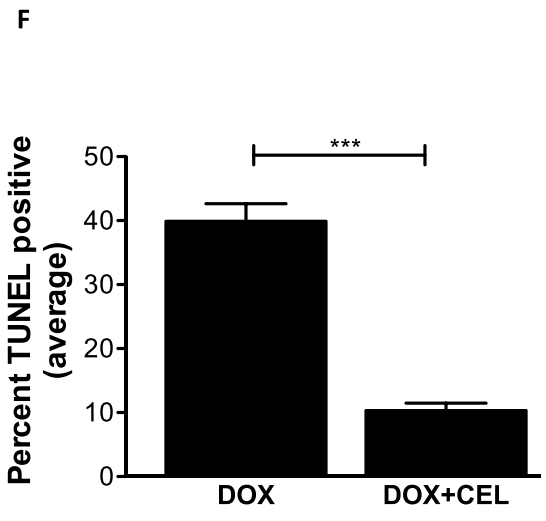

Fig. 1 Celastrol ameliorated DOX-induced cardiomyopathy and protected against myocardial ischemia injury

apoptotic events, we performed semiquantitative assay by TUNEL staining (Fig. 1e). A significantly higher number of TUNEL-positive cells (Fig. 1f) were detected in the DOX (n=7; 40±3 %) group as compared to the CEL + DOX (n=6; 10±2.2 %, ***P=0.0004) group. These results demonstrated that CEL treatment rescued the DOX-induced cardiomyopathy model by preventing cardiomyocyte apoptosis, preserving cardiac function and improving survival rates.

Celastrol protects against myocardial ischemia injury

Myocardial infarction triggers a volatile myocardial environment leading to cell death and compromised heart function due to activation of pro-inflammatory cytokines, apoptosis, and increased matrix metalloproteinase mediators (Kannaiyan et al. 2011). Mice were subjected to LAD ligation with CEL (MI + CEL group) or without CEL (MI group) treatment. Heart functionality was determined by left ventricle blood pool fractional area change in diastole (FAC, ejection fraction). Left ventricular ejection fractions (% LVEFs) were reduced in the MI group (31.45±4.99 at day 7 and 29.08±7.45 at day 28), but CEL treatment significantly improved the ejection fraction by 13 % at day 7 and 12 % at day 28 in the MI + CEL group (44.48±6.43 at day 7 and 41.9±5.24 at day 28) (Fig. 2a). We further quantified scar reduction in the myocardium by sections stained with Masson's trichrome to discern viable tissue from fibrous tissue at 28 days. A typical Masson staining pattern in hearts is shown in Fig. 2b. Viable myocardium was measured as a percentage of the LV circumference from trichrome-stained sections at 28 days post-MI surgery. Fewer purple-stained regions (viable tissue) were present in the MI hearts (CNT) within the predominately blue-stained (fibrous) infarct zone of heart sections. CEL treatment of MI hearts (Fig. 2c) increased the viable tissues (MI, n=6, 43.9±3.2 vs MI + CEL, n=6, 58.3±3.6 %, *P=0.026). We tested whether CEL suppressed inflammation resulting in decreased scar formation and improved cardiac function in a myocardial infarct model. As myocardial infarction causes high levels of inflammation, the inflammatory cell infiltration by monocytes and macrophages was determined by immunohistochemical staining for $CD68^+$ cells on the LV infarct section rings after 3 days of MI (Fig. 2d). Infiltration of $CD68^+$ cells in the border zone of LV after MI was significantly inhibited (MI, n=6, 9.2±1.0 vs MI + CEL, n=5, 5.0±1.3 %, *P=0.034) after CEL treatment (Fig. 2e). To further confirm myocardial inflammation, mRNA expression of various pro-inflammatory cytokines (TNF-α, IL-1β, and IL-6) were determined by quantitative RT-PCR in the myocardium at 3 days post-MI. Infarcted myocardium showed an increase of 4.7±0.5 in IL-6, 17.5±1.1 in IL-1β, and 5.8±1.1 in TNF-α folds in mRNA expression. However, CEL treatment of MI animals showed a significant reduction in the mRNA expression fold levels of pro-inflammatory cytokines (2.2±0.3 in IL-6, 9.5±1.4 in IL-1β, and 2.3±0.4 in TNF-α, Fig. 2f–h). Similar results were observed for MMP2 (Supplemental Fig. 2). Taken together, these results demonstrate that CEL preserved cardiac function in two different acute cardiomyopathy models. Importantly, CEL treatment showed no evidence of macroscopic or microscopic toxicity including the vital organs brain, liver, kidney, lungs, stomach, spleen, and pancreas (Supplemental Fig. 3). Clinical signs of body weight loss, change in behavior (aggression, hypermobility, and hunchback), discoloration of stool or urine, and fur loss or discoloration were not observed.

Fig. 2 Celastrol treatment preserved cardiac function after myocardial infarction. **a** Echocardiography was performed before MI and after 7 days or after 28 days which showed a preservation of function with CEL treatment (**P<0.01, *P<0.05, two-way ANOVA followed by Bonferroni's test). **b** A representative picture of Masson's trichrome staining of heart sections (*scale bar*=3.0 mm, magnification ×2.5). **c** Quantitative histological assessment of viable tissue at day 28 showed a reduced infarct expansion in CEL-treated mice as compared to controls (*P=0.026, Mann–Whitney test). **d** CEL treatment suppressed CD68-positive cell infiltration in the myocardium at 3 days post-MI by histological evaluation (*scale bar*=480 μm, magnification ×10). **e** Quantitative assessment showed a significant decrease in the number of $CD68^+$ cells in MI hearts after CEL treatment as compared to MI hearts (*P=0.034, Mann–Whitney test). **f**–**h** Quantitative analysis of inflammation-related cytokines and chemokines (*P<0.05, **P<0.01, *** P<0.001, Kruskal–Wallis test followed by Dunn's post hoc test). Data are represented as mean±SEM

Celastrol protects against thioacetamide-induced hepatotoxicity

We next tested the cytoprotective activity of celastrol in an acute thioacetamide (TAA)-induced liver inflammation model, representing another common human disease. TAA-treated mice had 100 % mortality by post-treatment day 4 due to acute liver failure; however, the TAA + CEL group reported an 86.7 % survival rate at post-treatment day 7 (Fig. 3a). The TAA group had liver appearances with palpably larger, harder granulo-nodules on the surface and obtuse liver edges, which were all consistent with acute liver dysfunction. The TAA + CEL group showed significantly improved liver appearance with smaller granulo-nodules and a smooth liver surface. Evaluated by hematoxylin–eosin staining, the TAA group showed extensive necrosis, marked bridging fibrosis, and thick fibrous septa compatible with acute liver failure, whereas the TAA + CEL group attenuated these alterations to just mild inflammation and occasional portal-to-portal bridging or perioral fibrosis (Fig. 3b). Apoptotic events in the liver were analyzed by performing semiquantitative assay by TUNEL staining (Fig. 3c). A significantly higher number of TUNEL-positive cells were detected in the TAA group than in the CEL + TAA group (TAA, n=5, 130±7.0 vs TAA + CEL, n=5, 9.0±2.0, *P=0.011, ***P<0.001, Fig. 3d). Analysis of the biochemical liver function parameters demonstrated

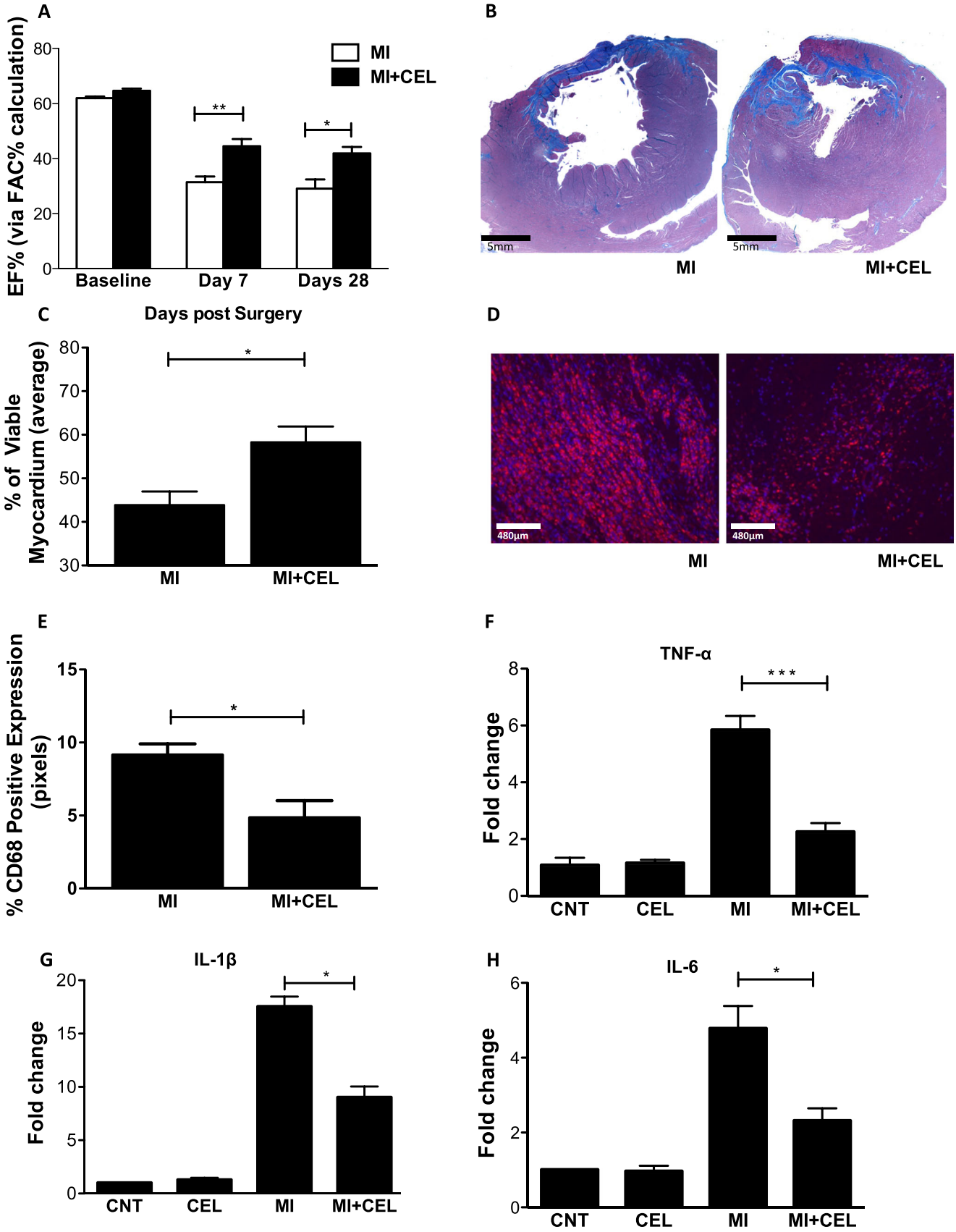
A
EF% (via FAC% calculation)
80
60
40
20
0
MI
MI+CEL
**
*
Baseline
Day 7
Days 28
B
5mm
5mm
MI
MI+CEL
C
Days post Surgery
% of Viable Myocardium (average)
80
70
60
50
40
30
*
MI
MI+CEL
D
480µm
480µm
MI
MI+CEL
E
% CD68 Positive Expression (pixels)
15
10
5
0
*
MI
MI+CEL
F
TNF-α
Fold change
8
6
4
2
0
***
CNT
CEL
MI
MI+CEL
G
IL-1β
Fold change
20
15
10
5
0
*
CNT
CEL
MI
MI+CEL
H
IL-6
Fold change
6
4
2
0
*
CNT
CEL
MI
MI+CEL

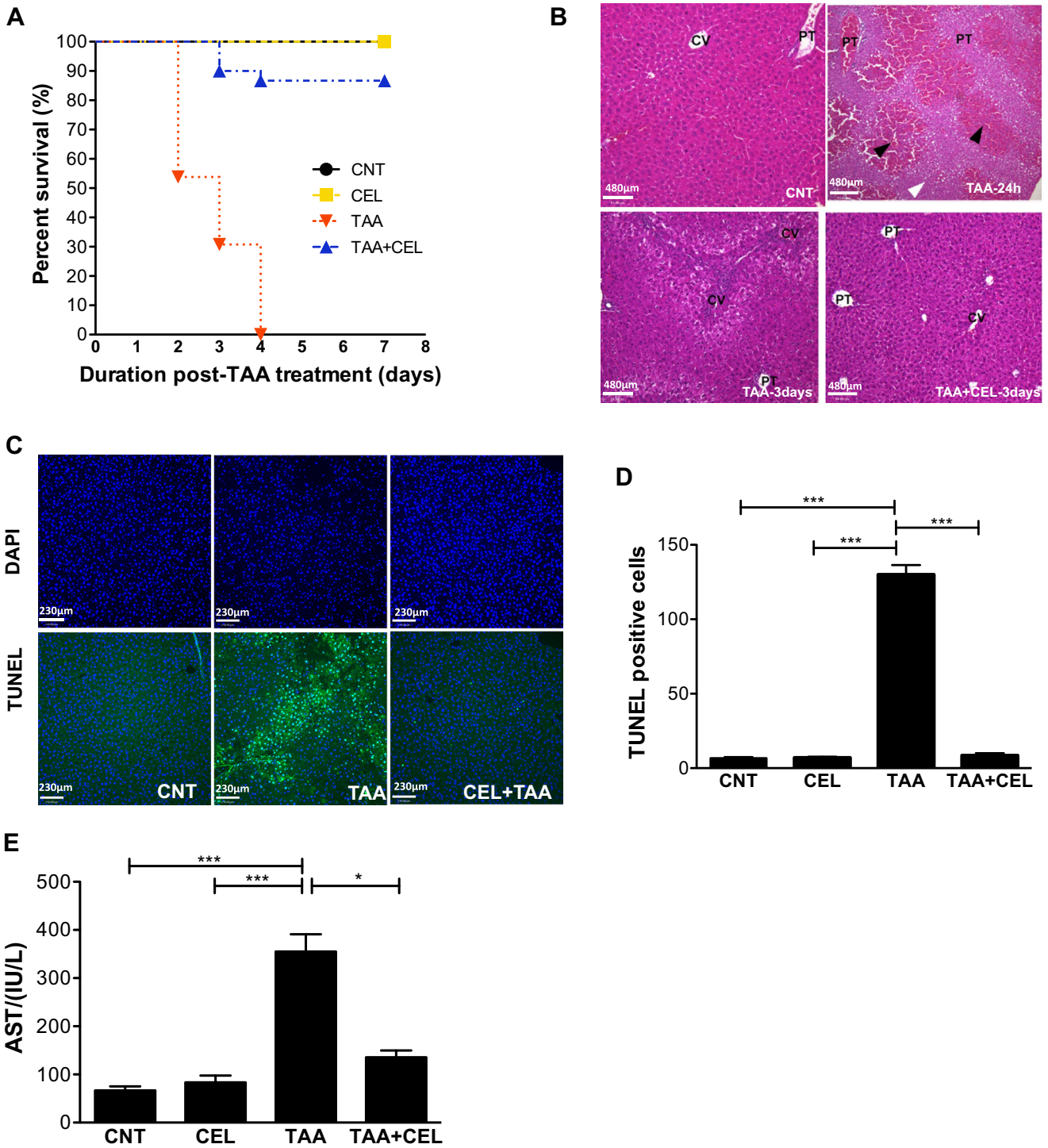

Fig. 3 Celastrol treatment enhanced survival after thioacetamide-induced liver toxicity in mice. **a** After TAA exposure, the CEL + TAA (n=9, 87 %) group when compared to the TAA group (n=8, 0 %, P<0.0001, log-rank (Mantel–Cox) test) had a significant survival rate by Kaplan–Meier plot. **b** TAA exposure showed lobular disorganization and CV hemorrhaging which was absent with CEL treatment (*PT* portal triad, *CV* central vein, *black arrowhead* hemorrhaging and necrotic liver parenchyma, *white arrowhead* normal undamaged hepatocytes, *scale bar*=480 μm, magnification ×10). **c** TUNEL apoptosis assays on liver sections obtained from untreated (control), TAA group, and TAA + CEL group. DAPI was used to counterstain nuclei. **d**. Quantitative analysis of TUNEL assay suggested that CEL treatment antagonized TAA exposure. TUNEL-positive nuclei are expressed as the average of five fields/sample (*scale bar*=230 μm, magnification ×20). **e** The AST levels were significantly elevated by TAA exposure but brought to normal levels with CEL treatment. Data are analyzed by one-way ANOVA, followed by Kruskal–Wallis test, and presented as mean±SEM

that the TAA + CEL group had significantly lower aspartate aminotransferase (AST) levels than the TAA group (TAA, n=9, 397±56.0 vs TAA + CEL, n=9, 124.0±33.0, *P=0.015, ***P<0.001, Fig. 3e). CEL treatment prevented TAA-induced acute liver injury by decreasing hepatocyte apoptosis, preserving hepatic function and improving survival rates.

Celastrol increased cell viability in vitro

To determine the effect of CEL treatment in vitro, we tested cell viability by MTT assay in H9c2 cardiomyocytes exposed to DOX and Huh7 hepatocytes exposed to TAA. DOX significantly reduced cell viability by (n=10, 27.9±2.5 %) in H9c2 cells, while CEL treatment increased cell viability in a dose-dependent manner with a peak recovery at a 100-nM CEL dose (CEL + DOX, n=10, 76.5±2.0 %, *P<0.05, **P<0.01, ***P<0.001) (Fig. 3a). Similarly, TAA treatment of Huh7 cells reduced the cell viability (n=6, 41.0±3.0 %) while CEL co-treatment of TAA-exposed Huh7 cells resulted in an increased cell viability with a peak recovery at a 300-nM CEL dose (n=6, 77±3.0 %, *P<0.05, ***P<0.001) (Fig. 3b). The optimal pretreatment timing for CEL was 24 h that increased maximum cell viability as shown in DOX-treated H9c2 cells (Supplemental Fig. 4a). To further validate efficacy, CEL treatment improved the cell viability curve with increasing doses of DOX (Supplemental Fig. 4b). We further determined whether CEL treatment decreased the apoptotic cells using Annexin V/PI staining by fluorescence-activated cell sorting (FACS). DOX increased the early apoptotic cells (R2) and total dead cells (R1 + R2) in the H9c2 cells (Supplemental Fig. 5). CEL reduced these cell populations to baselines to the same extent as those present in the CNT group. Importantly, CEL treatment alone had no noticeable effect on the number of apoptotic cells. We measured active caspase-3 activity as a downstream effector of apoptosis by immunohistochemical staining (Fig. 4c). Quantification analysis showed that the induction of cleaved caspase-3 activity in H9c2 (DOX, n=6, 72±6 % vs CEL + DOX, n=6, 33±8 %, **P=0.0087) and Huh7 cells (TAA, n=6, 64±6 % vs CEL + TAA, n=6, 31±4 %, *P=0.0043) was significantly reduced in the presence of CEL (Fig. 4d).

FACS analysis demonstrated that DOX increased active caspase-3 expression in H9c2 cells and CEL treatment reduced cleaved caspase-3 activity to significantly lower levels (DOX, n=7, 48±6.036 % vs DOX + CEL, n=7, 24±4 %, *P= 0.0156) (Fig. 4e). However, total recovery from DOX-induced caspase-3 activation was not achieved by CEL treatment. CEL alone had no effect on the level of active caspase-3. Similar observations were seen with CEL treatment in TAA-exposed Huh7 cells. TAA treatment increased active caspase-3 expression in Huh7 cells, but CEL treatment reduced cleaved caspase-3 activity (TAA, n=6, 63.3±6.86 % vs TAA + CEL, n=6, 31.5±5.1 %, *P= 0.0313) (Fig. 4f). We further checked the efficacy of CEL treatment in Huh7 cells in the presence of acetaminophen (APAP) as the treatment with DOX or TAA after 48 h results in 100 % cell death. Huh7 cells were treated with APAP in the presence or absence of CEL for 24, 48, and 96 h with media change (with or without CEL) every 24 h. Cells were immune-stained for cleaved caspase-3. CEL treatment inhibited caspase-3 activation in Huh7 cells up to 96 h in the presence of APAP treatment, suggesting the long-lasting efficacy of CEL (Fig. 4g).

Celastrol maintains expression of lineage-specific transcription factors

GATA4 is a cardiac-specific transcription factor, highly expressed in the heart and rapidly depleted in the presence of DOX (Aries et al. 2004). Overexpression of GATA4 prevents DOX-induced apoptosis in cardiomyocytes (Aries et al. 2004; Kim et al. 2003), suggesting that GATA4 depletion significantly contributes to DOX-induced apoptosis. Likewise, other lineage-specific transcriptional factors may play a crucial role in maintaining the lineage-specific protein profile and may have further anti-apoptotic effects similar to GATA4. For instance, Hnf-1α and Hnf-4α are crucial for the hepatocytes (DeLaForest et al. 2011; Hayhurst et al. 2001; Parviz et al. 2003; Quasdorff et al. 2008). Since CEL treatment regulates multiple transcriptional factors belonging to HSP90's clients in a cell-specific manner (Zhang et al. 2010), we next tested whether the expression of lineage-specific transcriptional factors fluctuated in the presence of CEL treatment during exposure to DOX or TAA. DOX exposure triggered a time-dependent reduction of GATA4 protein expression in H9c2 cardiomyocytes, and similarly, TAA reduced the expression of Hnf-1α and Hnf-4α protein expression in Huh7 cells (Fig. 5a, b). CEL treatment restored GATA4 protein levels in H9c2 cells and Hnf-1α and Hnf-4α protein levels in Huh7 cells, similar to levels present in controls (Fig. 5c, d). Quantitative PCR analysis showed that the RNA levels of cell-specific transcription factors, GATA4 in H9c2 cells after DOX insult, were also restored to levels present in control with CEL treatment (Supplemental Fig. 6). Taken together, these results suggest that CEL treatment maintained the lineage-specific transcriptional profile in the different cell types which maybe essential for their cell survival.

We next determined whether the cytoprotective activity of CEL correlated by activating HSPs. CEL treatment increased the protein levels of hsp70 and hsp27 in a dose-dependent manner in H9c2 cells (Fig. 5e) but showed no effect on the protein expression for hsp90 and hsp40. Similarly, hsp70 and HSP27 showed a decreased protein expression level in the presence of DOX-exposed H9c2. We next determined whether CEL treatment correlated with increased protein levels of hsp70, hsp27, and GATA4 in the DOX cardiomyopathy model in vivo. By day 5, DOX had decreased protein levels of

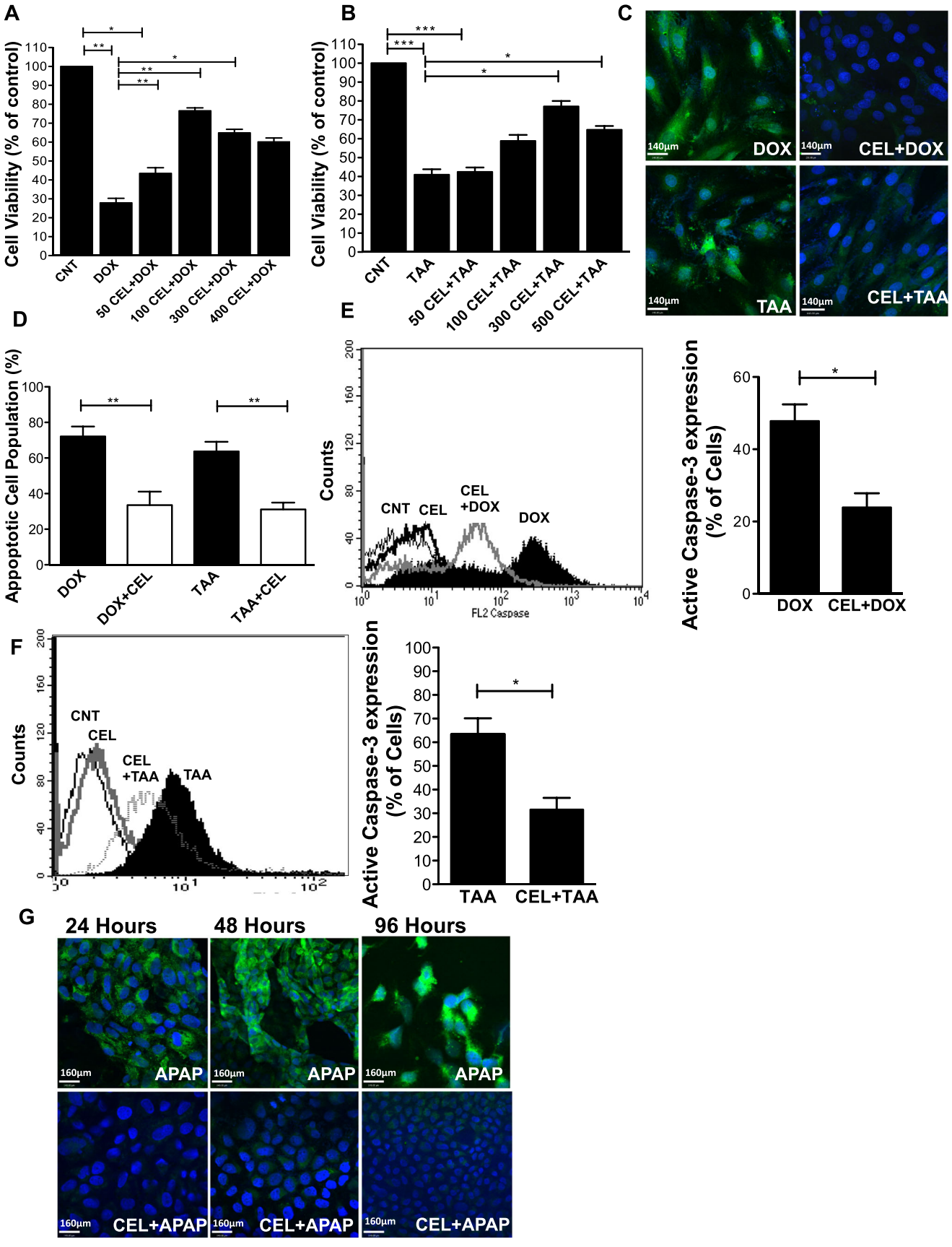
A
Cell Viability (% of control)
CNT
DOX
50 CEL+DOX
100 CEL+DOX
300 CEL+DOX
400 CEL+DOX
B
Cell Viability (% of control)
CNT
TAA
50 CEL+TAA
100 CEL+TAA
300 CEL+TAA
500 CEL+TAA
C
DOX
CEL+DOX
TAA
CEL+TAA
140µm
D
Appoptotic Cell Population (%)
DOX
DOX+CEL
TAA
TAA+CEL
E
Counts
CNT
CEL
CEL +DOX
DOX
FL2 Caspase
Active Caspase-3 expression (% of Cells)
DOX
CEL+DOX
F
Counts
CNT
CEL
CEL +TAA
TAA
Active Caspase-3 expression (% of Cells)
TAA
CEL+TAA
G
24 Hours
48 Hours
96 Hours
APAP
CEL+APAP
160µm

◀ **Fig. 4** Cell viability increased by CEL treatment against cytotoxins. **a** The cell viability of DOX-exposed H9c2 cells was significantly increased with CEL measured by MTT. **b**. The cell viability of TAA-exposed Huh7 cells was significantly increased with CEL. Data are analyzed by one-way ANOVA followed by Kruskal–Wallis test with Dunn's comparisons. **c** Immunostaining of DOX-exposed H9c2 cells and TAA-exposed Huh7 cells in the absence (*upper panel*) or presence (*lower panel*) of CEL showed an inhibition of active caspase-3 expression (*scale bar*=140 μm, magnification ×40). **d** Quantitative analysis of active caspase-3 expression showed a significant decrease in apoptotic cells with CEL (non-parametric *t* test followed by Mann–Whitney's analysis). **e** FACS analysis of active caspase-3 expression in H9c2 cells exposed to DOX and treated with CEL. **f** FACS analysis of active caspase-3 expression in and Huh7 cells exposed to TAA. After drug exposure by cytometric histogram plot (*left*) and quantitative analysis (*right*) showed a higher expression level of active caspase-3 in DOX- and TAA-exposed cells when compared in DOX + CEL or TAA + CEL. FACS data were analyzed by non-parametric *t* test followed by Mann–Whitney's analysis. **g** Immunostaining showed that APAP exposure resulted in almost complete cell death after 96 h, while in the presence of CEL, minimal cell death was observed (*scale bar*=160 μm, magnification ×40). Data are represented as mean±SEM)

GATA4 and hsp27 in comparison to controls (Fig. 5f). HSP70 protein level expression was minimally effected by DOX or CEL treatments. In contrast, CEL treatment preserved hsp27 and GATA4 protein expression in comparison to DOX treatment alone. Taken together, these results provide a strong correlation that CEL treatment maintained key lineage-specific transcriptional factors by activating HSPs.

HSR is necessary for the action of celastrol

We next performed three different experiments to determine whether the activation of HSR is necessary for the cytoprotective action of CEL treatment. We used $HSF1^{+/+}$ and $HSF1^{-/-}$ mouse embryonic fibroblast (MEF) cells and determined whether CEL restored cell viability after DOX exposure in these cells (McMillan et al. 2002; McMillan et al. 1998). DOX treatment significantly reduced cell viability in $HSF1^{+/+}$ MEF cells but was recovered with CEL treatment in a dose-dependent manner to a maximum recovery (DOX, n=8, 24±3 % vs DOX + CEL, n=8, 72±2 %, $^{**}P<0.01$, $^{***}P<0.001$) (Fig. 6a). In contrast, DOX treatment reduced the cell viability in $HSF1^{-/-}$ MEF cells but CEL treatment failed to improve cell viability, implicating that the HSF1 is necessary for the cells viability in CEL treatment (DOX, n=6, 46±1.5 % vs DOX + CEL, n=6, 48 ±3 %) (Fig. 6b). We further verified CEL treatment on inducing the HSR in the $HSF1^{+/+}$ and $HSF1^{-/-}$ MEF cells by examining the protein expression of hsp90, hsp70, hsp40, and hsp27 (Fig. 6c). In $HSF^{+/+}$ MEF cells, CEL failed to induce hsp90 and hsp40 protein levels but increased hsp70 and hsp27 protein levels in a dose-dependent manner. In $HSF1^{-/-}$ MEF cells, CEL treatment caused no increase in the protein levels of the HSPs levels tested (Fig. 6d). Taken together, these results demonstrated that CEL has a cytoprotective effect by activating HSF1 and subsequently hsp70 and hsp27 in vitro.

In the second experiment, we used selective knockdown approach using small interfering RNA (siRNA) targeting HSF1 in H9c2 as per the schematic shown in Fig. 6e. Quantitative immunoblot analysis and qRT-PCR demonstrated silencing of the hsf1 protein and RNA effectively to <5 % expression as compared to scrambled siRNA transfection in H9c2 (Supplemental Fig. 7). Next, we determined whether CEL treatment preserved GATA4 in HSF1-silenced, DOX-exposed H9c2 cells. In CEL + DOX-treated H9c2 cells, GATA4 protein levels were restored up to 65 % as compared to 25 % in DOX-alone-treated cells, but CEL treatment had no recovery in the HSF1 knockdown H9c2 cells (Fig. 6f, g).

The third experiment determined whether the HSR is necessary for the effect of CEL treatment in the DOX-induced cardiomyopathy model in vivo by using a chemical inhibitor of HSF1, triptolide (TTD) (Phillips et al. 2007; Westerheide et al. 2006; Whitesell and Lindquist 2009). We initially established that in vitro in the presence of DOX, CEL failed to recover GATA4 protein levels with TTD co-treatment due to decreased HSP70 activation (Fig. 6h). Similarly, co-treatment with TTD reduced the expression of hsp70, Hnf-1α, and Hnf-4α in Huh7 cells despite CEL treatment (Supplemental Fig. 8). Next, we performed survival experiments in the DOX-induced cardiomyopathy model in the presence of TTD. The results of survival experiments showed that the control, TTD, and CEL-alone groups were consistently at 100 % survival rate. The DOX group had a reduced survival rate to 25 %. Similarly, the CEL + TTD + DOX group had a reduced survival rate of 22 % but the CEL + DOX group once again had an 80 % survival rate (Fig. 6i). Taken together, these three experiments provide direct evidence that HSF1 is necessary and sufficient for the cytoprotective abilities of CEL.

Discussion

In this study, we sought to determine the ability of celastrol to treat three different animal disease models involving cardiomyopathy and liver failure. Our findings show that celastrol has a striking ability to decrease mortality in a DOX cardiomyopathy model and in a TAA-induced liver dysfunction model. Celastrol decreased the inflammation response and recovered the cardiac function in a MI model. The mechanism of this cytoprotection relies on the necessary activation of the HSR. By controlling this pathway, celastrol utilizes and enhances the protective cellular response that already exists within the cell.

One of the major findings of this study is the bioefficacy of orally administered celastrol in the three organs tested.

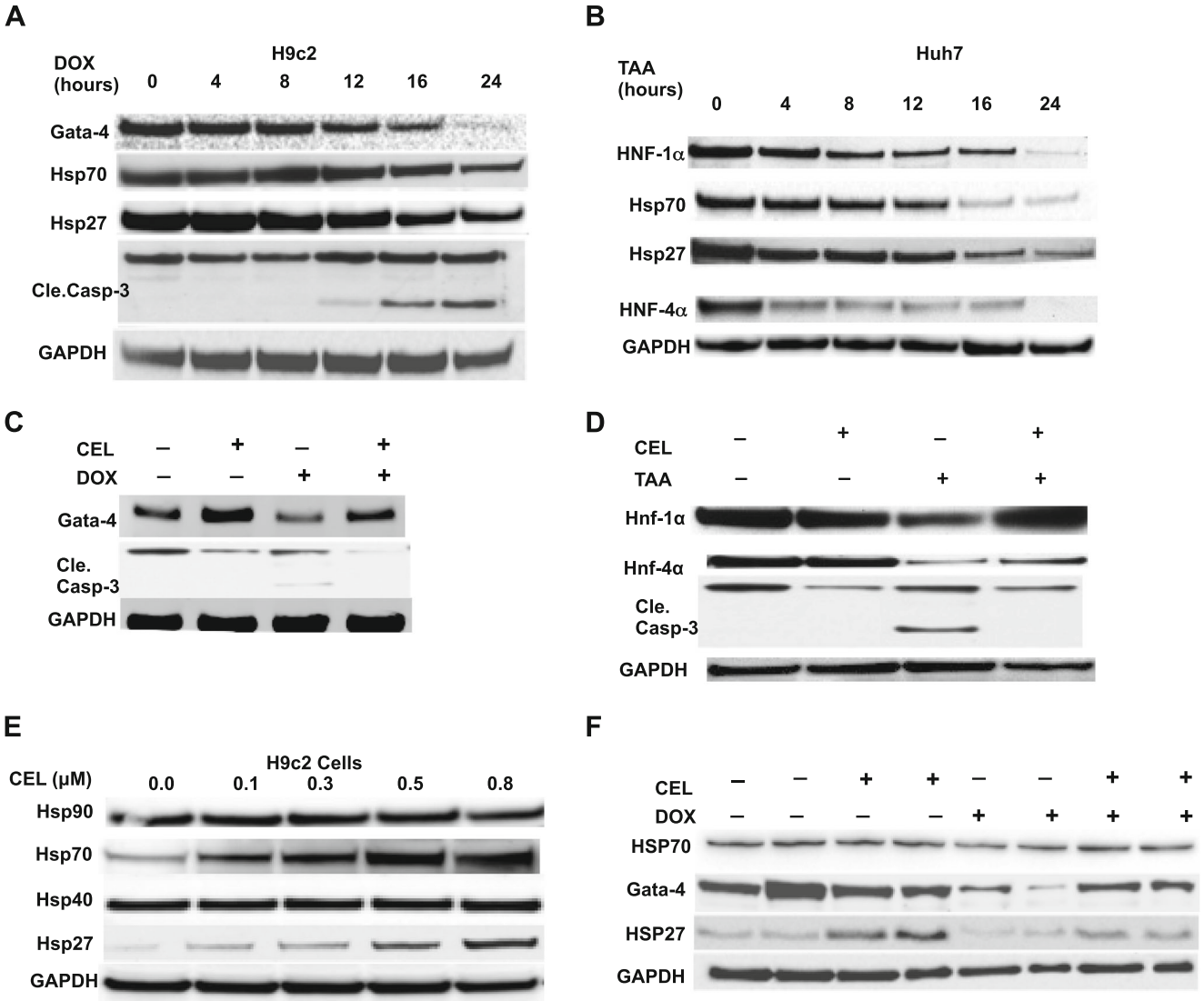

Fig. 5 Celastrol increased HSPs and preserved essential transcription factors. **a**, **b** Immunoblot analysis showed an increase in active caspase-3 expression after exposure to DOX and TAA in H9c2 and Huh7 cells, respectively. GATA4 in H9c2 and Hnf-1α and Hnf-4α in Huh7 cells were decreased in a time-dependent manner after exposure to DOX or TAA. **c**, **d** GATA4 protein expression in H9c2 cells and Hnf-1α and Hnf-4α protein levels in Huh7 cells were restored to normal levels after CEL treatment by immunoblot analysis. Cleaved caspase-3 expression was significantly reduced. **e** CEL treatment increased hsp70 and hsp27 without showing any effect on hsp90 and hsp40 in a dose-dependent manner by immunoblot analysis. **f** CEL treatment restored GATA4 and hsp27 protein levels in mice hearts after DOX exposure analyzed by immunoblot analysis

Previous studies have focused on single cellular pathways or have targeted overexpressing single HSPs that have invasive delivery routes of administration (Laflamme et al. 2007). In our study, we have determined the bioavailability for orally delivered celastrol using a mixture of Cremophor to allow for better gastrointestinal absorption. This is in contrast to a previous attempt of another celastrol oral preparation using polyethanol glycol, which had poor systemic absorption (Zhang et al. 2012). More importantly, celastrol has no tissue-specific selectivity, broad tissue penetrance, and limited side effect profile which make its general applications more appealing. No other small-molecule HSR activator has been shown to be delivered with such ease and efficacy. Lastly, the ability of celastrol to harness the innate cellular HSR machinery to prevent entire disease processes creates a universal application of this drug for many disease processes yet to be tested.

The mechanism by which orally delivered celastrol induces the HSR is unclear and needs further investigation. We provided evidence that the transactivation of HSF1 is necessary and sufficient for the bioactivity of celastrol. But exactly how celastrol transactivates HSF1 is unclear. More specifically, celastrol may inactivate HSP90, which then stimulates HSF1 transactivation, or another mechanism may involve the direct transactivation of HSF1. In support of the first possible mechanism, celastrol induced a transcriptional factor array similar

to what is reported for inactivating HSP90 in three human cell lines (Zhang et al. 2010). However, our data supports that celastrol does not change the protein expression level of hsp90 in our cell lines tested which may suggest that a post-translational modification of hsp90 modification may need to occur. Another mechanism for celastrol to increase the HSR may involve other pathways that indirectly increase hsf1 protein levels. One mechanism may occur by the inhibition of NF-κB pathway because many compounds that activate HSR also inhibit the NF-κB pathway, including celastrol (Chen 2011; Li-Weber 2013; Li et al. 2012; Shao et al. 2013; Westerheide et al. 2009). Another mechanism may involve celastrol activation of sirtulin that then deacetylates HSF1 in which state it binds more strongly to HSPs regulatory elements, allowing increased HSPs expression (Westerheide et al. 2009). Future investigations will be needed to elucidate how celastrol triggers the transactivation of HSF1.

Our observations demonstrate the striking ability of celastrol to treat three animal models involving different organs like the heart and liver. In the first model, celastrol protected the cardiomyocytes from apoptosis induced by DOX and thus improved the survival rate by 60 %. These results are consistent with previous studies that demonstrated that individual overexpression of hsp20, hsp27, hsp60, or hsp70 provided cardioprotection against DOX toxicity by modulating the Akt pathway or protection of aconitase from DOX-generated reactive oxygen species (Saxena et al. 2008). In the second model, celastrol protected cardiomyocytes from myocardial ischemia, improved LV function, and reduced scar formation. Other studies have also demonstrated that, individually, overexpression of HSPs have similar abilities to functionally recover the ischemic myocardium but relied on either direct activation of the HSR or transgenic mice overexpressing the HSPs (Marber et al. 1995; Mestril et al. 1994a; Mestril et al. 1994b; Plumier et al. 1995). In our experience, celastrol functionally recovered the injured ischemic myocardium to the same extent by measurement of ejection fraction when compared to resident cardiac stem cells ex vivo expanded and transplanted into the injured myocardium (Simpson et al. 2012, unpublished data). Celastrol may offer a non-invasive, non-cell-based therapy for improving left ventricle function after myocardial ischemia that may change the therapeutic approach in heart failure patients. Further studies will be needed to verify this possibility. Taken together, these results suggest the potent abilities of celastrol to preserve cellular injury regardless of the organ.

Celastrol is one of the most promising plant extracts that is highly therapeutic in many disease processes (Hu et al. 2013; Kannaiyan et al. 2011; Liu et al. 2011). Celastrol has been shown to ameliorate many disease processes involving neurodegenerative (Chen et al. 2014; Choi et al. 2014; Paul and Mahanta 2014), autoimmune (Grant et al. 2013; Kim et al. 2013; Venkatesha et al. 2012), and inflammatory diseases (Youn et al. 2014; Yu et al. 2010). Celastrol performs this effect through possibly many cellular processes that involves not only the HSR but also activating other innate survival pathways. For instance, it was recently shown that celastrol upregulates heme-oxygenase-1 to reduce myocardial infarct size and to functionally recover the myocardium in a myocardial infarcted animal model (Der Sarkissian et al. 2014). Celastrol-mediated cytoprotection through either activation of heme-oxygenase-1 (Francis et al. 2011; Hansen et al. 2011; Seo et al. 2011; Yu et al. 2010) or HSR or upregulation of other cellular processes needs further clarification to determine the contributory role each pathway plays in treating disease models.

The paradigm of HSR regulation has previously focused on gene-targeting activation of HSF1 or various key downstream HSPs (Kondo et al. 2011; Morimoto and Santoro 1998; Pirkkala et al. 2000; Pirkkala et al. 2001; Shi et al. 1998). Our results reveal that the network that regulates the HSR can be controlled with a single drug, celastrol. The HSR activates a large network, encompassing over 50 genes in response to various stressors (Morimoto 1998; Pirkkala et al. 2000; Pirkkala et al. 2001). Many of the genes have been previously linked to the HSR regulation in other systems including prokaryotes, suggesting the conserved evolution of this cellular response. The precise mechanism of how many of the genes interlink together to activate this cascade is unclear in the presence of celastrol and needs further defining. Furthermore, it will be important to determine how celastrol can influence other well-described, HSR-controlled processes, including cancer, ischemia-reperfusion, age-dependent human diseases, transplant surgery, and changes during development and during aging (Calderwood et al. 2009; Heydari et al. 1993; Terry et al. 2004; Terry et al. 2006). Since we have shown that the efficacy of celastrol is widely seen in the three different organs we tested, it will be important to determine whether celastrol has similar cytoprotective responses to toxic insults in other organs. We anticipate that celastrol now opens the opportunity to broadly activate the HSR in all tissue types, which may resist the body from potential lethal diseases.

In broader application, the HSR represents one pathway fundamental to cellular homeostasis. The major cellular homeostasis pathways are highly conserved in eukaryotic cells including all human tissue cells, which constitute about 1,000–2,000 proteins. These pathways are interconnected and provide the amazing dynamic range of functions that permits cells to maintain internal homeostasis in the face of external stressors. These pathways maintain a multitude of cellular processes involving ER stress, cellular protein folding and trafficking, oxidative stress, Ca^{+2} signaling, mTOR/autophagy, proteasomal activation, mitochondrial energy production, and heat shock induction. Conceptually, we can consider these pathways as connectors for a set of interconnected springs, which are the cellular

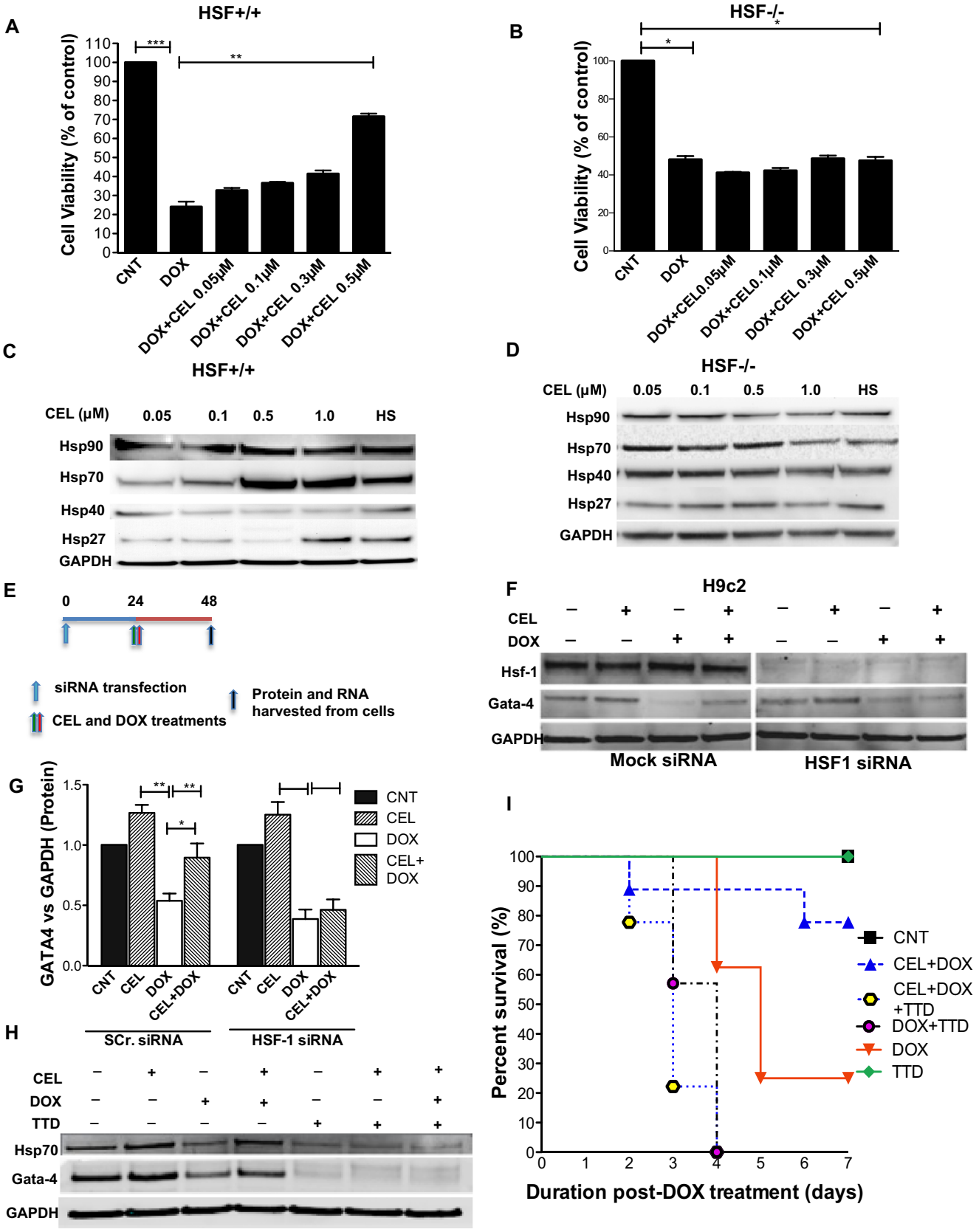
A
HSF+/+
Cell Viability (% of control)
CNT
DOX
DOX+CEL 0.05μM
DOX+CEL 0.1μM
DOX+CEL 0.3μM
DOX+CEL 0.5μM
B
HSF-/-
Cell Viability (% of control)
CNT
DOX
DOX+CEL0.05μM
DOX+CEL0.1μM
DOX+CEL 0.3μM
DOX+CEL 0.5μM
C
HSF+/+
CEL (μM) 0.05 0.1 0.5 1.0 HS
Hsp90
Hsp70
Hsp40
Hsp27
GAPDH
D
HSF-/-
CEL (μM) 0.05 0.1 0.5 1.0 HS
Hsp90
Hsp70
Hsp40
Hsp27
GAPDH
E
0 24 48
siRNA transfection
CEL and DOX treatments
Protein and RNA harvested from cells
F
H9c2
CEL
DOX
Hsf-1
Gata-4
GAPDH
Mock siRNA
HSF1 siRNA
G
GATA4 vs GAPDH (Protein)
CNT
CEL
DOX
CEL+ DOX
SCr. siRNA
HSF-1 siRNA
H
CEL
DOX
TTD
Hsp70
Gata-4
GAPDH
I
Percent survival (%)
Duration post-DOX treatment (days)
CNT
CEL+DOX
CEL+DOX +TTD
DOX+TTD
DOX
TTD

◀ **Fig. 6** The HSR is necessary for the cytoprotective action by celastrol. **a** Mouse embryonic fibroblasts (MEFs) were cultured with DOX in the presence or absence of CEL. Increasing CEL doses inhibited DOX toxicity measured by MTT assay. **b** CEL treatment could not inhibit DOX toxicity in $HSF1^{-/-}$ MEFs. **c**, **d** Immunoblot analysis showed that CEL treatment increased hsp70 and hsp27 without affecting hsp90 and hsp40 in $HSF1^{+/+}$ MEFS but not $HSF^{-/-}$ MEFs. **e** Knockdown of HSF1 by siRNA, drug administration, and sample collection were performed as outlined. **f** Immunoblot analysis of H9c2 cells with non-targeting siRNA showed that the depletion in GATA4 protein levels caused by DOX administration was restored to normal levels after treatment with CEL, while CEL failed to restore GATA4 protein levels in H9c2 cells targeted with HSF1 siRNA. **g** Quantification of GATA4 protein levels after mock siRNA and HSF1 siRNA transfection in H9c2 cells. **h** H9c2 cells were treated with triptolide (TTD) in the presence or absence of CEL treatment or DOX exposure as indicated for 18 h. Immunoblot analysis showed that the inhibition of HSP70 by TTD correlated with inhibition of GATA4 protein. **i** Survival rates were higher in the CEL + DOX group (n=9, 78 %) when compared to the DOX group (n=10, 25 %, P=0.0002, log-rank (Mantel–Cox) test) as shown by the Kaplan–Meier plot. TTD blocked the increased survival rate seen with CEL (CEL + TTD + DOX, n=9, 22 %). No mortality was observed in the CNT and TTD group

processes as stated above. When any external (e.g., a toxin or inciting protein or molecule) or internal (like a genetically altered and/or misfolded protein associated with a human disease) stressor impacts one of the springs, the other springs begin to vibrate so the cell can reach a homeostatic state that allows accommodation to the stressor, continued cellular function, and eventual cellular survival. If however the stressor overwhelms the dynamic capacity of this interconnected regulatory system, then the cellular breakdown leads to recognizable diseases. Celastrol is a first example of reestablishing the cellular homeostasis by oral administration.

In conclusion, we provide in this body of work that celastrol cytoprotects multiple organs in different disease models. Celastrol is easily delivered by oral administration with a high level of bioavailability. These observations suggest that there are certain stereotypical canonical events that are fundamental to many disease processes. We believe that versatile small molecules like celastrol will become important components to novel disease treatment strategy. Our proof-of-concept studies will allow us to rapidly translate these findings into meaningful clinical trials for disorders that await better treatment options.

Acknowledgments This work was supported by the following grants: National Institutes of Health (KO8HL097069) and the Thoracic Surgical Foundation for Research and Education.

References

Albanese V, Yam AY, Baughman J, Parnot C, Frydman J (2006) Systems analyses reveal two chaperone networks with distinct functions in eukaryotic cells. Cell 124:75–88. doi:10.1016/j.cell.2005.11.039

Allison AC, Cacabelos R, Lombardi VR, Alvarez XA, Vigo C (2001) Celastrol, a potent antioxidant and anti-inflammatory drug, as a possible treatment for Alzheimer's disease. Prog Neuro-Psychopharmacol Biol Psychiatry 25:1341–1357

Aries A, Paradis P, Lefebvre C, Schwartz RJ, Nemer M (2004) Essential role of GATA-4 in cell survival and drug-induced cardiotoxicity. Proc Natl Acad Sci U S A 101:6975–6980

Bagatell R, Paine-Murrieta GD, Taylor CW, Pulcini EJ, Akinaga S, Benjamin IJ, Whitesell L (2000) Induction of a heat shock factor 1-dependent stress response alters the cytotoxic activity of hsp90-binding agents. Clin Cancer Res : Off J Am Assoc Cancer Res 6:3312–3318

Balch WE, Morimoto RI, Dillin A, Kelly JW (2008) Adapting proteostasis for disease intervention. Science 319:916–919. doi:10.1126/science.1141448

Brown CR, Hong-Brown LQ, Welch WJ (1997) Correcting temperature-sensitive protein folding defects. J Clin Invest 99:1432–1444. doi:10.1172/JCI119302

Calderwood SK, Murshid A, Prince T (2009) The shock of aging: molecular chaperones and the heat shock response in longevity and aging—a mini-review. Gerontology 55:550–558

Chang FR et al (2003) Antitumor agents. 228. Five new agarofurans reissantins A-E, and cytotoxic principles from Reissantia buchananii. J Nat Prod 66:1416–1420. doi:10.1021/np030241v

Chen S (2011) Natural products triggering biological targets—a review of the anti-inflammatory phytochemicals targeting the arachidonic acid pathway in allergy asthma and rheumatoid arthritis. Curr Drug Targets 12:288–301

Chen S et al (2014) Celastrol prevents cadmium-induced neuronal cell death via targeting JNK and PTEN-Akt/mTOR network. J Neurochem 128:256–266. doi:10.1111/jnc.12474

Choi BS, Kim H, Lee HJ, Sapkota K, Park SE, Kim S, Kim SJ (2014) Celastrol from 'Thunder God Vine' protects SH-SY5Y cells through the preservation of mitochondrial function and inhibition of p38 MAPK in a rotenone model of Parkinson's disease. Neurochem Res 39:84–96

Cohen FE, Kelly JW (2003) Therapeutic approaches to protein-misfolding diseases. Nature 426:905–909. doi:10.1038/nature02265

Dai Y et al (2010) Natural proteasome inhibitor celastrol suppresses androgen-independent prostate cancer progression by modulating apoptotic proteins and NF-kappaB. PLoS One 5:e14153. doi:10.1371/journal.pone.0014153

DeLaForest A, Nagaoka M, Si-Tayeb K, Noto FK, Konopka G, Battle MA, Duncan SA (2011) HNF4A is essential for specification of hepatic progenitors from human pluripotent stem cells. Development 138:4143–4153

Der Sarkissian S et al. (2014) Celastrol protects ischemic myocardium through heat shock response with upregulation of heme oxygenase-1. British journal of pharmacology doi:10.1111/bph.12838

Deuerling E, Bukau B (2004) Chaperone-assisted folding of newly synthesized proteins in the cytosol. Crit Rev Biochem Mol Biol 39:261–277. doi:10.1080/10409230490892496

Dohi E et al (2012) Hypoxic stress activates chaperone-mediated autophagy and modulates neuronal cell survival. Neurochem Int 60:431–442. doi:10.1016/j.neuint.2012.01.020

Francis SP, Kramarenko, II, Brandon CS, Lee FS, Baker TG, Cunningham LL (2011) Celastrol inhibits aminoglycoside-induced ototoxicity via heat shock protein 32. Cell death & disease 2:e195 doi:10.1038/cddis.2011.76

Grant CW, Moran-Paul CM, Duclos SK, Guberski DL, Arreaza-Rubin G, Spain LM (2013) Testing agents for prevention or reversal of type 1 diabetes in rodents. PLoS One 8:e72989

Hansen J, Palmfeldt J, Vang S, Corydon TJ, Gregersen N, Bross P (2011) Quantitative proteomics reveals cellular targets of celastrol. PLoS One 6:e26634. doi:10.1371/journal.pone.0026634

Hayhurst GP, Lee YH, Lambert G, Ward JM, Gonzalez FJ (2001) Hepatocyte nuclear factor 4alpha (nuclear receptor 2A1) is essential for maintenance of hepatic gene expression and lipid homeostasis. Mol Cell Biol 21:1393–1403

Heydari AR, Wu B, Takahashi R, Strong R, Richardson A (1993) Expression of heat shock protein 70 is altered by age and diet at the level of transcription. Mol Cell Biol 13:2909–2918

Hightower LE (1980) Cultured animal cells exposed to amino acid analogues or puromycin rapidly synthesize several polypeptides. J Cell Physiol 102:407–427. doi:10.1002/jcp.1041020315

Holmberg CI, Illman SA, Kallio M, Mikhailov A, Sistonen L (2000) Formation of nuclear HSF1 granules varies depending on stress stimuli. Cell Stress Chaperones 5:219–228

Hoogstra-Berends F et al (2012) Heat shock protein-inducing compounds as therapeutics to restore proteostasis in atrial fibrillation. Trends Cardiovasc Med 22:62–68. doi:10.1016/j.tcm.2012.06.013

Hu Y, Wang S, Wu X, Zhang J, Chen R, Chen M, Wang Y (2013) Chinese herbal medicine-derived compounds for cancer therapy: a focus on hepatocellular carcinoma. J Ethnopharmacol 149:601–612. doi:10.1016/j.jep.2013.07.030

Huot J, Roy G, Lambert H, Chretien P, Landry J (1991) Increased survival after treatments with anticancer agents of Chinese hamster cells expressing the human Mr 27,000 heat shock protein. Cancer Res 51:5245–5252

Imai J, Yashiroda H, Maruya M, Yahara I, Tanaka K (2003) Proteasomes and molecular chaperones: cellular machinery responsible for folding and destruction of unfolded proteins. Cell Cycle 2:585–590

Jaattela M, Wissing D (1992) Emerging role of heat shock proteins in biology and medicine. Ann Med 24:249–258

Jaattela M, Wissing D, Bauer PA, Li GC (1992) Major heat shock protein hsp70 protects tumor cells from tumor necrosis factor cytotoxicity. EMBO J 11:3507–3512

Jung HW, Chung YS, Kim YS, Park YK (2007) Celastrol inhibits production of nitric oxide and proinflammatory cytokines through MAPK signal transduction and NF-kappaB in LPS-stimulated BV-2 microglial cells. Exp Mol Med 39:715–721. doi:10.1038/emm.2007.78

Jurivich DA, Sistonen L, Kroes RA, Morimoto RI (1992) Effect of sodium salicylate on the human heat shock response. Science 255:1243–1245

Kannaiyan R, Shanmugam MK, Sethi G (2011) Molecular targets of celastrol derived from Thunder of God Vine: potential role in the treatment of inflammatory disorders and cancer. Cancer Lett 303:9–20. doi:10.1016/j.canlet.2010.10.025

Kaufman RJ (2002) Orchestrating the unfolded protein response in health and disease. J Clin Invest 110:1389–1398. doi:10.1172/JCI16886

Kim DH, Shin EK, Kim YH, Lee BW, Jun JG, Park JH, Kim JK (2009a) Suppression of inflammatory responses by celastrol, a quinone methide triterpenoid isolated from Celastrus regelii. Eur J Clin Investig 39:819–827

Kim DY, Park JW, Jeoung D, Ro JY (2009b) Celastrol suppresses allergen-induced airway inflammation in a mouse allergic asthma model. Eur J Pharmacol 612:98–105. doi:10.1016/j.ejphar.2009.03.078

Kim JE et al (2013) Celastrol, an NF-kappaB inhibitor, improves insulin resistance and attenuates renal injury in db/db mice. PLoS One 8:e62068

Kim Y et al (2003) Anthracycline-induced suppression of GATA-4 transcription factor: implication in the regulation of cardiac myocyte apoptosis. Mol Pharmacol 63:368–377

Kondo T, Koga S, Matsuyama R, Miyagawa K, Goto R, Kai H, Araki E (2011) Heat shock response regulates insulin sensitivity and glucose homeostasis: pathophysiological impact and therapeutic potential. Curr diabetes Rev 7:264–269

Kubo M et al (2012) Heat shock factor 1 contributes to ischemia-induced angiogenesis by regulating the mobilization and recruitment of bone marrow stem/progenitor cells. PLoS One 7:e37934

Laflamme MA et al (2007) Cardiomyocytes derived from human embryonic stem cells in pro-survival factors enhance function of infarcted rat hearts. Nat Biotechnol 25:1015–1024. doi:10.1038/nbt1327

Lee BS, Chen J, Angelidis C, Jurivich DA, Morimoto RI (1995) Pharmacological modulation of heat shock factor 1 by antiinflammatory drugs results in protection against stress-induced cellular damage. Proc Natl Acad Sci U S A 92:7207–7211

Li-Weber M (2013) Targeting apoptosis pathways in cancer by Chinese medicine. Cancer Lett 332:304–312. doi:10.1016/j.canlet.2010.07.015

Li K et al (2006) Thrombopoietin protects against in vitro and in vivo cardiotoxicity induced by doxorubicin. Circulation 113:2211–2220. doi:10.1161/CIRCULATIONAHA.105.560250

Li Y et al (2012) Protective effect of celastrol in rat cerebral ischemia model: down-regulating p-JNK, p-c-Jun and NF-kappaB. Brain Res 1464:8–13

Lis J, Wu C (1993) Protein traffic on the heat shock promoter: parking, stalling, and trucking along. Cell 74:1–4

Liu Z, Ma L, Zhou GB (2011) The main anticancer bullets of the Chinese medicinal herb, thunder god vine. Mol (Basel, Switzerland) 16:5283–5297

Marber MS, Mestril R, Chi SH, Sayen MR, Yellon DM, Dillmann WH (1995) Overexpression of the rat inducible 70-kD heat stress protein in a transgenic mouse increases the resistance of the heart to ischemic injury. J Clin Invest 95:1446–1456

McMillan DR et al (2002) Heat shock transcription factor 2 is not essential for embryonic development, fertility, or adult cognitive and psychomotor function in mice. Mol Cell Biol 22:8005–8014

McMillan DR, Xiao X, Shao L, Graves K, Benjamin IJ (1998) Targeted disruption of heat shock transcription factor 1 abolishes thermotolerance and protection against heat-inducible apoptosis. J Biol Chem 273:7523–7528

Mehlen P, Kretz-Remy C, Briolay J, Fostan P, Mirault ME, Arrigo AP (1995a) Intracellular reactive oxygen species as apparent modulators of heat-shock protein 27 (hsp27) structural organization and phosphorylation in basal and tumour necrosis factor alpha-treated T4ss human carcinoma cells. Biochem J 312(Pt 2):367–375

Mehlen P, Preville X, Chareyron P, Briolay J, Klemenz R, Arrigo AP (1995b) Constitutive expression of human hsp27, Drosophila hsp27, or human alpha B-crystallin confers resistance to TNF- and oxidative stress-induced cytotoxicity in stably transfected murine L929 fibroblasts. J Immunol 154:363–374

Mestril R, Chi SH, Sayen MR, Dillmann WH (1994a) Isolation of a novel inducible rat heat-shock protein (HSP70) gene and its expression during ischaemia/hypoxia and heat shock. Biochem J 298(Pt 3):561–569

Mestril R, Chi SH, Sayen MR, O'Reilly K, Dillmann WH (1994b) Expression of inducible stress protein 70 in rat heart myogenic cells confers protection against simulated ischemia-induced injury. J Clin Invest 93:759–767

Minino AM (2013) Death in the United States, 2011 NCHS data brief:1–8

Mishra R et al (2011) Characterization and functionality of cardiac progenitor cells in congenital heart patients. Circulation 123:364–373. doi:10.1161/CIRCULATIONAHA.110.971622

Mizzen LA, Welch WJ (1988) Characterization of the thermotolerant cell. I. Effects on protein synthesis activity and the regulation of heat-shock protein 70 expression. J Cell Biol 106:1105–1116

Morimoto RI (1993) Cells in stress: transcriptional activation of heat shock genes. Science 259:1409–1410

Morimoto RI (1998) Regulation of the heat shock transcriptional response: cross talk between a family of heat shock factors, molecular chaperones, and negative regulators. Genes Dev 12:3788–3796

Morimoto RI, Santoro MG (1998) Stress-inducible responses and heat shock proteins: new pharmacologic targets for cytoprotection. Nat Biotechnol 16:833–838. doi:10.1038/nbt0998-833

Mosser DD, Kotzbauer PT, Sarge KD, Morimoto RI (1990) In vitro activation of heat shock transcription factor DNA-binding by

calcium and biochemical conditions that affect protein conformation. Proc Natl Acad Sci U S A 87:3748–3752
Mu TW, Ong DS, Wang YJ, Balch WE, Yates JR 3rd, Segatori L, Kelly JW (2008) Chemical and biological approaches synergize to ameliorate protein-folding diseases. Cell 134:769–781. doi:10.1016/j.cell.2008.06.037
Nagai N, Nakai A, Nagata K (1995) Quercetin suppresses heat shock response by down regulation of HSF1. Biochem Biophys Res Commun 208:1099–1105. doi:10.1006/bbrc.1995.1447
Niforou K, Cheimonidou C, Trougakos IP (2014) Molecular chaperones and proteostasis regulation during redox imbalance. Redox Biology 2:323–332. doi:10.1016/j.redox.2014.01.017
Parsell DA, Kowal AS, Lindquist S (1994) Saccharomyces cerevisiae Hsp104 protein purification and characterization of ATP-induced structural changes. Jo biol Chem 269:4480–4487
Parviz F et al (2003) Hepatocyte nuclear factor 4alpha controls the development of a hepatic epithelium and liver morphogenesis. Nat Genet 34:292–296
Paul S, Mahanta S (2014) Association of heat-shock proteins in various neurodegenerative disorders: is it a master key to open the therapeutic door? Mol Cell Biochem 386:45–61. doi:10.1007/s11010-013-1844-y
Phillips PA et al (2007) Triptolide induces pancreatic cancer cell death via inhibition of heat shock protein 70. Cancer Res 67:9407–9416. doi:10.1158/0008-5472.CAN-07-1077
Pinna GF, Fiorucci M, Reimund JM, Taquet N, Arondel Y, Muller CD (2004) Celastrol inhibits pro-inflammatory cytokine secretion in Crohn's disease biopsies. Biochem Biophys Res Commun 322:778–786. doi:10.1016/j.bbrc.2004.07.186
Pirkkala L, Alastalo TP, Zuo X, Benjamin IJ, Sistonen L (2000) Disruption of heat shock factor 1 reveals an essential role in the ubiquitin proteolytic pathway. Mol Cell Biol 20:2670–2675
Pirkkala L, Nykanen P, Sistonen L (2001) Roles of the heat shock transcription factors in regulation of the heat shock response and beyond. FASEB J : Off Publ Fed Am Soc Exp Biol 15:1118–1131
Plumier JC, Ross BM, Currie RW, Angelidis CE, Kazlaris H, Kollias G, Pagoulatos GN (1995) Transgenic mice expressing the human heat shock protein 70 have improved post-ischemic myocardial recovery. J Clin Invest 95:1854–1860
Pulitano C, Aldrighetti L (2008) The protective role of steroids in ischemia-reperfusion injury of the liver. Curr Pharm Des 14:496–503
Quasdorff M et al (2008) A concerted action of HNF4alpha and HNF1alpha links hepatitis B virus replication to hepatocyte differentiation. Cell Microbiol 10:1478–1490
Ron D, Walter P (2007) Signal integration in the endoplasmic reticulum unfolded protein response. Nat Rev Mol Cell Biol 8:519–529. doi:10.1038/nrm2199
Saxena A et al (2008) Stromal cell-derived factor-1alpha is cardioprotective after myocardial infarction. Circulation 117:2224–2231
Seo WY et al (2011) Celastrol induces expression of heme oxygenase-1 through ROS/Nrf2/ARE signaling in the HaCaT cells. Biochem Biophys Res Commun 407:535–540
Sethi G, Ahn KS, Pandey MK, Aggarwal BB (2007) Celastrol, a novel triterpene, potentiates TNF-induced apoptosis and suppresses invasion of tumor cells by inhibiting NF-kappaB-regulated gene products and TAK1-mediated NF-kappaB activation. Blood 109:2727–2735
Shao L et al (2013) Celastrol suppresses tumor cell growth through targeting an AR-ERG-NF-kappaB pathway in TMPRSS2/ERG fusion gene expressing prostate cancer. PLoS One 8:e58391
Shi Y, Mosser DD, Morimoto RI (1998) Molecular chaperones as HSF1-specific transcriptional repressors. Genes Dev 12:654–666
Simpson DL, Mishra R, Sharma S, Goh SK, Deshmukh S, Kaushal S (2012) A strong regenerative ability of cardiac stem cells derived from neonatal hearts. Circulation 126:S46–S53. doi:10.1161/CIRCULATIONAHA.111.084699
Terry DF et al (2004) Cardiovascular disease delay in centenarian offspring: role of heat shock proteins. Ann N Y Acad Sci 1019:502–505. doi:10.1196/annals.1297.092
Terry DF et al (2006) Serum heat shock protein 70 level as a biomarker of exceptional longevity. Mech Ageing Dev 127:862–868
Trott A, West JD, Klaic L, Westerheide SD, Silverman RB, Morimoto RI, Morano KA (2008) Activation of heat shock and antioxidant responses by the natural product celastrol: transcriptional signatures of a thiol-targeted molecule. Mol Biol Cell 19:1104–1112. doi:10.1091/mbc.E07-10-1004
Tucker NR, Middleton RC, Le QP, Shelden EA (2011) HSF1 is essential for the resistance of zebrafish eye and brain tissues to hypoxia/reperfusion injury. PLoS One 6:e22268
Venkatesha SH, Astry B, Nanjundaiah SM, Yu H, Moudgil KD (2012) Suppression of autoimmune arthritis by Celastrus-derived Celastrol through modulation of pro-inflammatory chemokines. Bioorg Med Chem 20:5229–5234. doi:10.1016/j.bmc.2012.06.050
Westerheide SD, Anckar J, Stevens SM Jr, Sistonen L, Morimoto RI (2009) Stress-inducible regulation of heat shock factor 1 by the deacetylase SIRT1. Science 323:1063–1066. doi:10.1126/science.1165946
Westerheide SD et al (2004) Celastrols as inducers of the heat shock response and cytoprotection. J Biol Chem 279:56053–56060. doi:10.1074/jbc.M409267200
Westerheide SD, Kawahara TL, Orton K, Morimoto RI (2006) Triptolide, an inhibitor of the human heat shock response that enhances stress-induced cell death. J Biol Chem 281:9616–9622
Whitesell L, Lindquist S (2009) Inhibiting the transcription factor HSF1 as an anticancer strategy. Expert Opin Ther Targets 13:469–478
Youn GS, Kwon DJ, Ju SM, Rhim H, Bae YS, Choi SY, Park J (2014) Celastrol ameliorates HIV-1 Tat-induced inflammatory responses via NF-kappaB and AP-1 inhibition and heme oxygenase-1 induction in astrocytes. Toxicology and applied pharmacology doi:10.1016/j.taap.2014.07.010
Young JC, Agashe VR, Siegers K, Hartl FU (2004) Pathways of chaperone-mediated protein folding in the cytosol. Nat Rev Mol Cell Biol 5:781–791. doi:10.1038/nrm1492
Yu X, Tao W, Jiang F, Li C, Lin J, Liu C (2010) Celastrol attenuates hypertension-induced inflammation and oxidative stress in vascular smooth muscle cells via induction of heme oxygenase-1. Am J Hypertens 23:895–903. doi:10.1038/ajh.2010.75
Zhang D, Xu L, Cao F, Wei T, Yang C, Uzan G, Peng B (2010) Celastrol regulates multiple nuclear transcription factors belonging to HSP90's clients in a dose- and cell type-dependent way. Cell Stress Chaperones 15:939–946. doi:10.1007/s12192-010-0202-1
Zhang J, Li CY, Xu MJ, Wu T, Chu JH, Liu SJ, Ju WZ (2012) Oral bioavailability and gender-related pharmacokinetics of celastrol following administration of pure celastrol and its related tablets in rats. J Ethnopharmacol 144:195–200. doi:10.1016/j.jep.2012.09.005